J. Fluid Mech. (2026), *vol.* 1033, R5, doi:10.1017/jfm.2026.11466

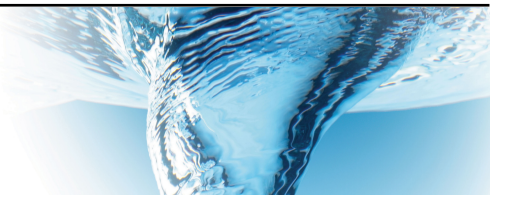

Effects of bulk viscosity on statistical scaling in compressible isotropic turbulence

Yiming Qi[1], **Jie Shen**[2], **Lian-Ping Wang**[2], **Tianbai Xiao**[1], **Jianchun Wang**[2], **Yonghao Zhang**[1] **and Shiyi Chen**[3,4]

[1]Centre for Interdisciplinary Research in Fluids, Institute of Mechanics, Chinese Academy of Sciences, Beijing 100190, PR China

[2]Guangdong Provincial Key Laboratory of Turbulence Research and Applications, Center for Complex Flows and Soft Matter Research and Department of Mechanics and Aerospace Engineering, Southern University of Science and Technology, Shenzhen, Guangdong 518055, PR China

[3]Eastern Institute for Advanced Study, Eastern Institute of Technology, Ningbo, Zhejiang 315200, PR China

[4]State Key Laboratory for Turbulence and Complex Systems, College of Engineering, Peking University, Beijing 100871, PR China

Corresponding author: Yiming Qi, 11610204@mail.sustech.edu.cn

(Received 1 December 2025; revised 16 February 2026; accepted 22 March 2026)

We perform numerical simulations of forced homogeneous isotropic turbulence over a range of bulk viscosities, Reynolds numbers and Mach numbers to investigate the scaling of key flow statistics. Using the Helmholtz decomposition, we analyse the scalings of Favre-averaged turbulent kinetic energy (TKE), root-mean-square (r.m.s.) pressure, pressure dilatation, dilatational dissipation and higher-order velocity-gradient moments. Additionally, new models are proposed for the pressure-dilatation term and the bulk-viscosity dependence of dilatational dissipation. Although the solenoidal and dilatational components of the Favre-averaged TKE are not strictly orthogonal, our numerical results demonstrate that their ratio is well approximated by the squared ratio of the corresponding r.m.s. velocities. The r.m.s. pressure approaches the pseudo-sound scaling as bulk viscosity increases. Within the Donzis r.m.s. pressure model (Donzis & John 2020 *Phys. Rev. Fluids* **5**(8), 084609), we find that the solenoidal contribution becomes dominant for large bulk viscosity. Pressure dilatation is found to depart systematically from pseudo-sound predictions: without bulk viscosity it favours transfer from kinetic to internal energy, while finite bulk viscosity can reverse this transfer at high Mach numbers. The scaling exponent of dilatational dissipation is shown to vary with bulk viscosity, enabling a corrected model for its exponent and prefactor. Velocity-gradient skewness and flatness reveal that the onset of shocklet-induced divergence is delayed with increasing bulk viscosity and may

be suppressed entirely. The results extend recent velocity-ratio-based scaling frameworks and provide modelling insights into compressible turbulence.

Key words: compressible turbulence, isotropic turbulence, turbulence theory

1. Introduction

Universal scaling remains a central pursuit in turbulence research, with homogeneous isotropic turbulence serving as a canonical framework that retains the essential dynamics while avoiding complications from inhomogeneity and boundaries. In incompressible flows, the Taylor-microscale Reynolds number Re_λ characterises the turbulence. In compressible turbulence, however, interactions among vortical, acoustic and entropic modes (Kovásznay 1953; Chu & Kovásznay 1958) render Re_λ alone insufficient. For fixed thermophysical parameters, including the specific heat ratio γ and Prandtl number Pr, conventional theory typically predicts normalised statistics as functions of Re_λ and the turbulent Mach number Ma_t. In compressible homogeneous isotropic turbulence, the two governing parameters are defined as

$$Re_\lambda = \frac{u_{rms}\lambda\langle\rho\rangle}{\langle\mu\rangle}, \quad Ma_t = \frac{\sqrt{3}u_{rms}}{\langle\sqrt{\gamma RT}\rangle}, \tag{1.1}$$

where ρ is the density, μ is the shear viscosity, R is the specific gas constant, T is the temperature, $u_{rms} = \sqrt{\langle u^2\rangle/3}$ is the root-mean-square (r.m.s.) velocity, λ is the Taylor microscale λ and angular brackets are suitably defined ensemble averages. The Helmholtz decomposition (Helmholtz 1867) uniquely separates the velocity field into two orthogonal components, namely $\boldsymbol{u} = \boldsymbol{u}_s + \boldsymbol{u}_d$; the divergence-free solenoidal velocity $\boldsymbol{u}_s$ (i.e. $\boldsymbol{\nabla}\cdot\boldsymbol{u}_s = 0$) is associated with the vortical mode, and the irrotational dilatational velocity $\boldsymbol{u}_d$ (i.e. $\boldsymbol{\nabla}\times\boldsymbol{u}_d = \boldsymbol{0}$) is related to the change rate of the volume element. Donzis & John (2020) demonstrated that self-similar scaling in compressible turbulence requires the consideration of dilatational motion. And they introduced the ratio of the r.m.s. dilatational velocity $u_{d,rms} = \sqrt{\langle u_d^2\rangle/3}$ to the r.m.s. solenoidal velocity $u_{s,rms} = \sqrt{\langle u_s^2\rangle/3}$. This velocity-ratio framework provides a more universal scaling and has since been extended to mean shear, thermal, reactive (Donzis & John 2020; John & Donzis 2024), magnetohydrodynamic (Li *et al.* 2024) and bulk-viscosity flows.

Pressure may also be decomposed into solenoidal and dilatational components, i.e. $p = p_s + p_d$ (Donzis & John 2020). Unlike the turbulent kinetic energy (TKE) per unit mass $\langle u^2\rangle/2 = \langle u_s^2\rangle/2 + \langle u_d^2\rangle/2$, whose solenoidal–dilatational split is exact, the square of the r.m.s. pressure $p_{rms}^2 = p_{s,rms}^2 + p_{d,rms}^2 + 2r_p\, p_{s,rms}\, p_{d,rms}$ has an additional contribution from the correlation coefficient r_p between p_s and p_d. Dilatational pressure p_d reflects an acoustic dynamics with a characteristic time scale $t \sim 1/(c_s|\boldsymbol{\nabla}|)$ corresponding to the dilatational length scale $1/|\boldsymbol{\nabla}|$ ($\boldsymbol{\nabla}$ is the nabla operator of the spatial derivative), and the speed of sound $c_s = \sqrt{\gamma\langle p\rangle/\langle\rho\rangle}$. From mass conservation, the r.m.s. dilatational pressure satisfies $p_{d,rms}/\langle p\rangle \sim \gamma Ma_d$ (Donzis & John 2020), where $Ma_d = u_{d,rms}Ma_t/u_{rms}$ is the dilatational turbulent Mach number. The pressure Poisson equation further yields $p_{s,rms} \sim \langle\rho\rangle u_{s,rms}^2$ in the incompressible limit. Within the pressure decomposition framework, scaling with respect to Ma_d becomes clear: when p_s dominates, $p_{rms}/\langle p\rangle \sim \gamma Ma_d^2 u_{s,rms}^2/u_{d,rms}^2$, whereas dilatational dominance gives $p_{rms}/\langle p\rangle \sim \gamma Ma_d$, the so-called dilatationally dominated p-equipartition (DDE) regime (Donzis & John 2020).

Modelling the dissipation in compressible turbulence requires understanding of the pressure-dilatation term $\langle p\vartheta \rangle$ and dilatational dissipation $\epsilon_d = (\chi + 4/3)\langle \mu \vartheta^2 \rangle / \langle \rho \rangle$, where $\vartheta = \boldsymbol{\nabla} \cdot \boldsymbol{u}$ is the dilatation, and $\chi = \mu_V / \mu$ is the bulk-to-shear viscosity ratio. Conventional pseudo-sound theory (Ristorcelli 1995, 1997; Ristorcelli & Blaisdell 1997) forecasts both terms to scale with Ma_t^2. Within this framework, $\langle p\vartheta \rangle$, which characterises the interconversion between TKE and internal energy, is assumed to scale with the product of Ma_t^2 and the solenoidal dissipation $\epsilon_s = \langle \mu \omega^2 \rangle / \langle \rho \rangle$ in isotropic turbulence (Sarkar 1992; Ristorcelli 1995, 1997; Ristorcelli & Blaisdell 1997), where $\boldsymbol{\omega} = \boldsymbol{\nabla} \times \boldsymbol{u}$ denotes the vorticity. Similarly, ϵ_d satisfies $\epsilon_d / \epsilon_s \sim Ma_t^2 + O(Ma_t^4)$ (Sarkar *et al.* 1991; Ristorcelli 1997; Ristorcelli & Blaisdell 1997). A more recent approach (Donzis & John 2020) relates ϵ_d / ϵ_s to the velocity ratio $u_{d,rms}/u_{s,rms}$, with direct numerical simulations (DNSs) (Donzis & John 2020; John & Donzis 2024) supporting the scaling $\epsilon_d / \epsilon_s \sim u_{d,rms}^2 / u_{s,rms}^2$. This result extends the Ma_t-based conventional theory and offers new insight into compressible turbulence modelling. However, the dependence of $\langle p\vartheta \rangle$ on the velocity ratio remains unexplored.

High-order moments of the velocity field exhibit unique phenomena associated with $u_{d,rms}/u_{s,rms}$ for compressible turbulence. The skewness S_u and flatness F_u, i.e.

$$S_u = \frac{\left\langle \left[(\partial u_x/\partial x)^3 + (\partial u_y/\partial y)^3 + (\partial u_z/\partial z)^3 \right]/3 \right\rangle}{\left\langle \left[(\partial u_x/\partial x)^2 + (\partial u_y/\partial y)^2 + (\partial u_z/\partial z)^2 \right]/3 \right\rangle^{3/2}}, \tag{1.2}$$

$$F_u = \frac{\left\langle \left[(\partial u_x/\partial x)^4 + (\partial u_y/\partial y)^4 + (\partial u_z/\partial z)^4 \right]/3 \right\rangle}{\left\langle \left[(\partial u_x/\partial x)^2 + (\partial u_y/\partial y)^2 + (\partial u_z/\partial z)^2 \right]/3 \right\rangle^{2}}, \tag{1.3}$$

which are closely related to vortex stretching and intermittency, deviate markedly from the canonical values observed in fully developed incompressible turbulence once $Ma_t u_{d,rms}^2 / u_{s,rms}^2$ exceeds a critical threshold, as a consequence of the emergence of intense shocklets (Samtaney, Pullin & Kosović 2001; Wang *et al.* 2011). When the so-called, S_u divergence, occurs, John & Donzis (2024) conjectured that it signifies the onset of a regime where dilatational motions begin to influence the turbulent energy cascade.

The dynamics of dilatational kinetic energy depends on several mechanisms, with bulk viscosity μ_V exerting a particularly strong influence. The bulk viscosity of a gas is strongly correlated with its internal degrees of freedom; for example, χ at 300 K is 0.73 for N_2, 7.4 for water vapour, 30 for H_2 and as high as 3000 for CO_2 (Cramer 2012). As a thermophysical property, μ_V enhances the dissipation of dilatational motions and thereby mitigates flow compressibility (Pan & Johnsen 2017). Increasing μ_V leads the velocity ratio to scale as Ma_t^2 up to turbulent Mach numbers of 0.6 (Chen *et al.* 2019). Sakurai & Ishihara (2023, 2024) showed that the dilatational energy spectrum exhibits a k^{-3} power-law scaling at high wavenumbers, which is attributed to the presence of shocklets. As μ_V increases, both the amplitude of the high-wavenumber dilatational spectrum and the associated k^{-3} scaling are progressively suppressed. Despite its relevance, the robustness of established turbulence-scaling behaviours under varying bulk viscosity has not been systematically assessed. To address this issue, we conduct numerical simulations to investigate how bulk viscosity affects the universality of key scaling relations. We examine the scaling of p_{rms} across μ_V, propose χ-dependent modifications for $\langle p\vartheta \rangle$ and ϵ_d and show that the threshold associated with the onset of the 'S_u divergence' increases with χ. These results highlight the regulatory role of bulk viscosity in modulating the evolution of compressible turbulence.

2. Numerical details

Numerical simulations of the Navier–Stokes–Fourier equations are performed using the hybrid method developed by Wang *et al.* (2010), which combines a seventh-order weighted essentially non-oscillatory (WENO) scheme with an eighth-order compact finite-difference scheme. The governing equations follow the macroscopic formulation of Qi *et al.* (2023), as detailed in the supplemental material is available at https://doi.org/10.1017/jfm.2026.11466, and the numerical method solves the conservative form of the total energy equation. Here, we emphasise that the results presented here do not constitute a DNS in the strict sense, since strong shocks with a thickness smaller than the grid spacing are not directly resolved but are effectively modelled through the inherent numerical subgrid dissipation of the WENO scheme. The viscous stress in the momentum equation is

$$\boldsymbol{\sigma} = \mu\big[\nabla \boldsymbol{u} + (\nabla \boldsymbol{u})^T + (\chi - 2/3)\vartheta \boldsymbol{I}\big], \tag{2.1}$$

where μ satisfies Sutherland,s law (Sutherland 1893), a superscript T denotes the transpose for the velocity gradient and $\boldsymbol{I}$ is the identity tensor. To mitigate the impact of dilatational forcing (Petersen & Livescu 2010), solenoidal large-scale forcing is applied by maintaining prescribed kinetic energies in the two lowest-wavenumber shells, consistent with the $k^{-5/3}$ spectrum. The specific heat ratio and Prandtl number are set to $\gamma = 1.4$ and $Pr = 0.7$, respectively.

Table 1 in the supplementary material summarises the key parameters and statistical quantities for the simulations, which cover the parameter ranges of $Re_\lambda \in (99, 181)$, $Ma_t \in (0.39, 1.04)$ and $\chi \in [0, 30]$. The Taylor microscale λ and Kolmogorov scale η, along with the two parts of the Favre-averaged TKE, K_s and K_d, the r.m.s. vorticity ω_{rms} and dilation ϑ_{rms}, the integral time scale L_I, eddy-turnover time T_e and kinetic energy spectrum E_K are defined as

$$\lambda = \frac{\sqrt{3}u_{rms}}{\sqrt{\langle(\partial u_x/\partial x)^2 + (\partial u_y/\partial y)^2 + (\partial u_z/\partial z)^2\rangle}},\ \eta = \left[\frac{\langle\mu/\rho\rangle^3}{\varepsilon}\right]^{1/4},$$

$$K_s = \frac{\langle\rho u_s^2\rangle}{2\langle\rho\rangle},\ K_d = \frac{\langle\rho u_d^2\rangle}{2\langle\rho\rangle},\ \omega_{rms} = \sqrt{\langle\boldsymbol{\omega}\cdot\boldsymbol{\omega}\rangle},\ \vartheta_{rms} = \sqrt{\langle\vartheta^2\rangle},$$

$$L_I = \frac{\pi}{2u_{rms}^2}\int_0^\infty \frac{E_K(k)}{k}\mathrm{d}k,\ T_e = \frac{L_I}{u_{rms}},\ E_K(k,t) = \sum_{k-\frac{1}{2}<|\boldsymbol{k}|\leqslant k+\frac{1}{2}} \frac{|\hat{\boldsymbol{u}}(\boldsymbol{k},t)|^2}{2}, \tag{2.2}$$

with $\hat{\boldsymbol{u}}$ denoting the Fourier-transformed velocity in the wavenumber space $\boldsymbol{k}$. Stationary ensemble statistics are obtained from spatial averages with additional temporal averaging over more than $28T_e$. All simulations satisfy $k_{max}\eta > 2.27$, ensuring convergence of high-order velocity-gradient moments (Wang, Gotoh & Watanabe 2017).

3. Results

3.1. *Favre-averaged velocity decomposition*

In compressible turbulence modelling, the TKE is typically defined using the Favre (density-weighted) average. We therefore begin by analysing the solenoidal and dilatational Favre-averaged components, K_s and K_d. Although this decomposition is not orthogonal $\langle\rho\boldsymbol{u}_s\cdot\boldsymbol{u}_c\rangle \neq 0$, figure 1(*a*) shows that K_d/K_s collapses onto $u_{d,rms}^2/u_{s,rms}^2$ for all cases, demonstrating that the Favre-averaged TKE ratio provides a reliable proxy for

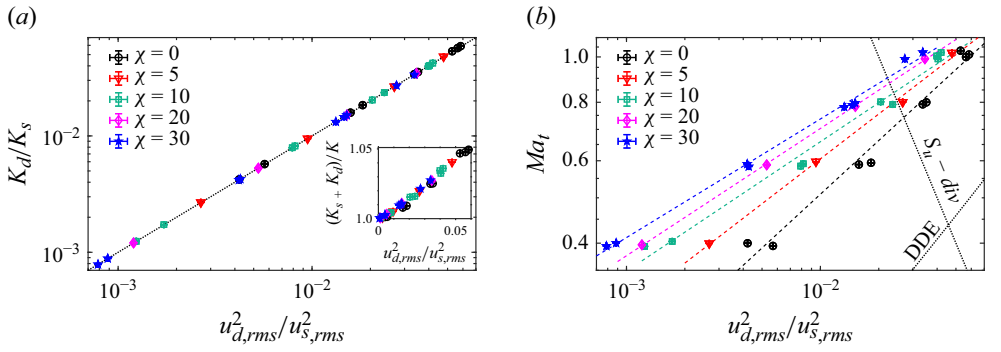

Figure 1. (*a*) Scaling of K_d/K_s vs. $u^2_{d,rms}/u^2_{s,rms}$ and (*b*) $Ma_t - u^2_{d,rms}/u^2_{s,rms}$ diagram. Data are represented as the 'mean ± standard error, in all figures.

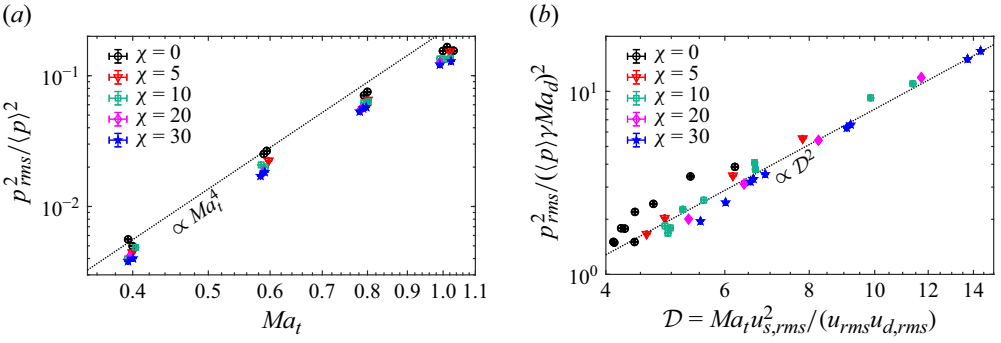

Figure 2. Scaling of (*a*) $p^2_{rms}/\langle p\rangle^2$ with Ma_t and (*b*) $p^2_{rms}/(\langle p\rangle \gamma Ma_d)^2$ with $\mathcal{D}$.

the velocity ratio under the present density-variation conditions. Besides, the inset in figure 1(*a*) shows that approximating K by $K_s + K_d$ yields deviations within 5 %, with the discrepancy increasing at higher velocity ratios.

The $Ma_t - u^2_{d,rms}/u^2_{s,rms}$ diagram in figure 1(*b*) includes two established criteria. The 'DDE' line ($\mathcal{D} = Ma_t u^2_{s,rms}/(u_{rms}u_{d,rms}) > 0.5$) (Donzis & John 2020) indicates that all cases lie in the solenoidal-pressure-dominated regime, with solenoidal contributions strengthened at larger bulk viscosity. The '$S_u - div$' line ($Ma_t u^2_{d,rms}/u^2_{s,rms} > 3 \times 10^{-2}$) (John & Donzis 2024) suggests that several simulations satisfy the empirical onset condition. Regarding the scaling of the turbulent Mach number, Donzis & John (2020) proposed that solenoidally forced isotropic turbulence may follow $Ma_t \sim C(u_{d,rms}/u_{s,rms})^{\alpha}$, with the same exponent α, while most of the cases they examined assume a zero bulk viscosity. By contrast, our results demonstrate a pronounced dependence of α on the bulk viscosity. The exponent decreases systematically with increasing χ and is well described by the empirical relation $\alpha \approx (0.460\chi + 4.57)/(\chi + 5.99)$.

3.2. *Pressure*

Figure 2(*a*) shows the variation of the normalised r.m.s. pressure $p^2_{rms}/\langle p\rangle^2$ with Ma_t. Classical pseudo-sound theory (Ristorcelli 1997; Donzis & Jagannathan 2013; Wang *et al.* 2017) predicts a quartic scaling $p^2_{rms}/\langle p\rangle^2 \sim Ma_t^4$, yet the measured exponents are consistently smaller than four. As χ increases, however, the scaling gradually

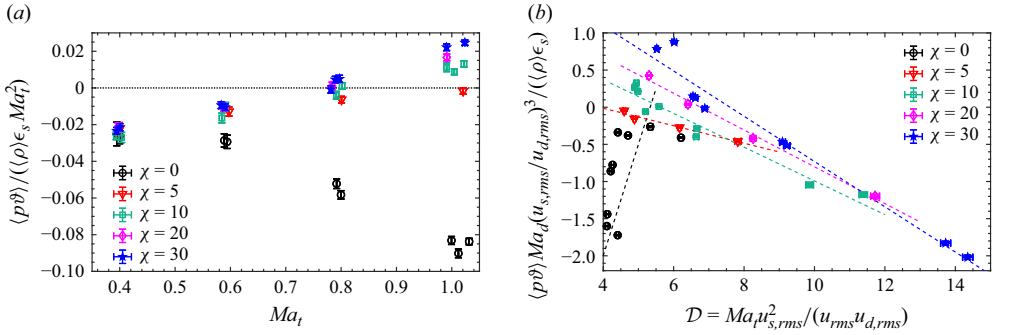

Figure 3. Scaling of (*a*) $\langle p\vartheta\rangle/(\langle\rho\rangle\epsilon_s Ma_t^2)$ with Ma_t and (*b*) $\langle p\vartheta\rangle Ma_d(u_{s,rms}/u_{d,rms})^3/(\langle\rho\rangle\epsilon_s)$ with $\mathcal{D}$.

approaches the quartic law. This trend can be attributed to the underlying pressure-generation mechanisms: pseudo-sound theory derives from the pressure Poisson equation at the incompressible limit, which reflects primarily solenoidal contributions. Elevated bulk viscosity suppresses dilatational motions, thereby enhancing the relative weight of solenoidal pressure and driving the overall behaviour closer to the pseudo-sound prediction. A unified representation of r.m.s. pressure was proposed by Donzis & John (2020), through a decomposition into solenoidal and dilatational components

$$\frac{p_{rms}^2}{(\langle p\rangle\gamma Ma_d)^2} \approx C_1\, Ma_d^2 \frac{u_{s,rms}^4}{u_{d,rms}^4} + C_2 = C_1\mathcal{D}^2 + C_2, \tag{3.1}$$

where $\mathcal{D} = Ma_d u_{s,rms}^2/u_{d,rms}^2 = Ma_t u_{s,rms}^2/(u_{rms}u_{d,rms})$ is the reciprocal of that defined in Donzis & John (2020). and the first term captures the solenoidal contribution while the second represents dilatational pressure. The detailed derivations of (3.1)–(3.3) are provided in the supplementary material. Figure 2(*b*) indicates that the normalised r.m.s. pressure follows the $\mathcal{D}^2$ scaling reasonably well with $C_1 \approx 0.08$ and $C_2 \approx 0$, and the agreement improves markedly with increasing χ, further confirming that the pressure field becomes progressively solenoidal-dominated when bulk-viscosity effects are strong.

3.3. *Dissipation*

We first examine the pressure-dilatation term $\langle p\vartheta\rangle$, representing the net work of pressure on a fluid element. In homogeneous isotropic turbulence, positive ϑ converts internal energy to TKE, while negative ϑ transfers TKE to internal energy. Figure 3(*a*) shows that the classical pseudo-sound scaling $\langle p\vartheta\rangle/\langle\rho\rangle\epsilon_s \sim Ma_t^2$ (Sarkar 1992) is not supported; the data display a stronger Mach-number dependence. Notably, with zero bulk viscosity ($\chi = 0$), the transfer is strictly from TKE to internal energy, whereas for $\chi \geqslant 5$ internal-to-TKE transfer appears at higher Mach numbers.

Based on the velocity ratio, an alternative model is constructed for $\langle p\vartheta\rangle$. Following the methodology of Zeman (1991), we rewrite the term as $\langle p\vartheta\rangle \approx -\langle(p_s + p_d)\partial p_d/\partial t\rangle/\gamma\langle p\rangle$ and simplify using the acoustic time scale $t \sim 1/(c_s|\nabla|)$, the solenoidal dissipation $\epsilon_s \approx u_{s,rms}^3/\mathcal{L}$ in the equilibrium turbulence (Kolmogorov 1941*a*,*b*; Rubinstein & Clark 2017) and the aforementioned model for p_{rms} (Donzis & John 2020),

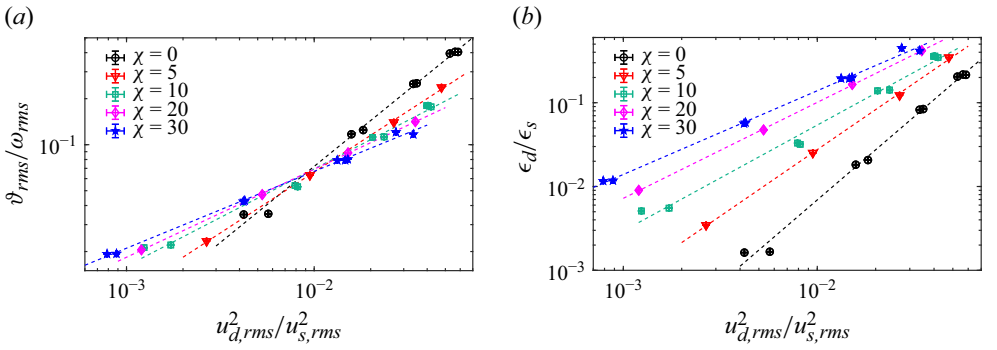

Figure 4. Scaling of (*a*) $\vartheta_{rms}/\omega_{rms}$ and (*b*) ϵ_d/ϵ_s with $u^2_{d,rms}/u^2_{s,rms}$.

leading to the relations

$$\langle p\vartheta\rangle \approx -\frac{c_s|\nabla|}{\gamma\langle p\rangle}\left(r_p\, p_{s,rms}\, p_{d,rms} + p^2_{d,rms}\right) = \langle\rho\rangle c_s^3|\nabla|Ma_d^2\,(C_3\mathcal{D}+C_4), \tag{3.2}$$

$$\frac{\langle p\vartheta\rangle}{\langle\rho\rangle\epsilon_s} \approx \mathcal{L}|\nabla|\frac{c_s^3}{u^3_{s,rms}}Ma_d^2\,(C_3\mathcal{D}+C_4) = \mathcal{L}|\nabla|\left(\frac{u_{d,rms}}{u_{s,rms}}\right)^3\frac{C_3\mathcal{D}+C_4}{Ma_d}, \tag{3.3}$$

where $\mathcal{L}$ is the energy-containing scale with the undetermined coefficients C_3 and C_4. As shown in figure 3(*b*), the model (represented by the line of the same colour) performs poorly for $\chi = 0$, consistent with the same limitations of the p_{rms} models (figure 2*b*), but agreement improves systematically as bulk viscosity increases. $\mathcal{L}|\nabla|$ may vary with Re_λ and Ma_t, warranting further study.

Figure 4(*a*) shows the dependence of $\vartheta_{rms}/\omega_{rms}$ on $u^2_{d,rms}/u^2_{s,rms}$. For a given bulk viscosity, the data follow a clear scaling $\vartheta_{rms}/\omega_{rms} \sim (u_{d,rms}/u_{s,rms})^\beta$, with the exponent β decreasing as χ increases, indicating non-zero bulk viscosity alters the dilatational motions rather than simply rescaling for flows without bulk viscosity. This trend suggests that the ratio ϵ_d/ϵ_s should likewise depend on the velocity ratio. Figure 4(*b*) confirms this, showing that ϵ_d/ϵ_s collapses onto an empirical relation of the form

$$\frac{\epsilon_d}{\epsilon_s} \approx C_5\left(\frac{u_{d,rms}}{u_{s,rms}}\right)^{2C_6},\ \lg C_5 = \frac{0.927\chi+18.6}{\chi+10.2},\ C_6 = \frac{0.694\chi+18.9}{\chi+9.46},\ \chi\in[0,30]. \tag{3.4}$$

Notably, the exponent C_6 for all simulated cases consistently exceeds the empirical value of unity proposed by Donzis & John (2020) and John & Donzis (2024), and our coefficients may be influenced by the finite dataset and should therefore be regarded as provisional. Increasing χ substantially amplifies the dilatational-dissipation contribution, demonstrating that ϵ_d cannot be neglected in compressible flows with large bulk viscosity.

3.4. *High-order velocity statistics*

Finally, we examine higher-order statistics of the velocity gradient, namely the skewness S_u and flatness F_u. The former reflects the vortex-stretching dynamics (Champagne 1978), whereas the latter characterises the turbulent intermittency (Pope 2000). In incompressible turbulence, both quantities exhibit only weak Re_λ dependence, with empirical scalings (Ishihara *et al.* 2007): $-S_u = (0.32\pm0.02)Re_\lambda^{0.11\pm0.01}$ and $F_u = (1.14\pm0.19)Re_\lambda^{0.34\pm0.03}$. In compressible flows, however, previous studies (Donzis & John 2020) suggest that, once

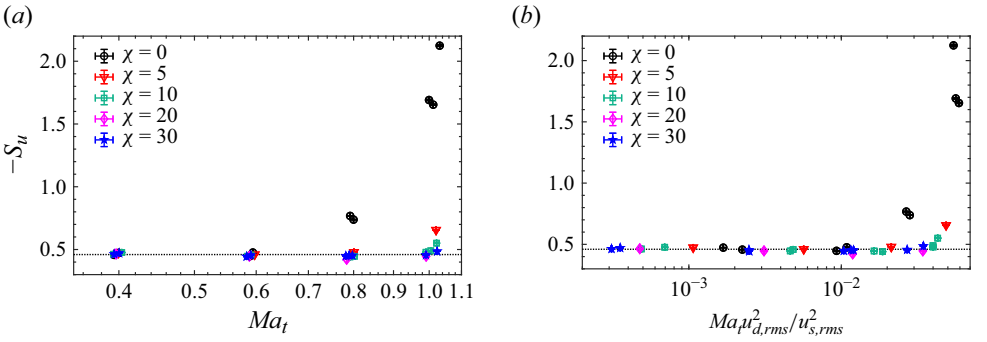

Figure 5. Skewness of the velocity gradient S_u with (*a*) Ma_t and (*b*) $Ma_t u^2_{d,rms}/u^2_{s,rms}$. The dotted line is the average value 0.460 for the cases before S_u-divergence.

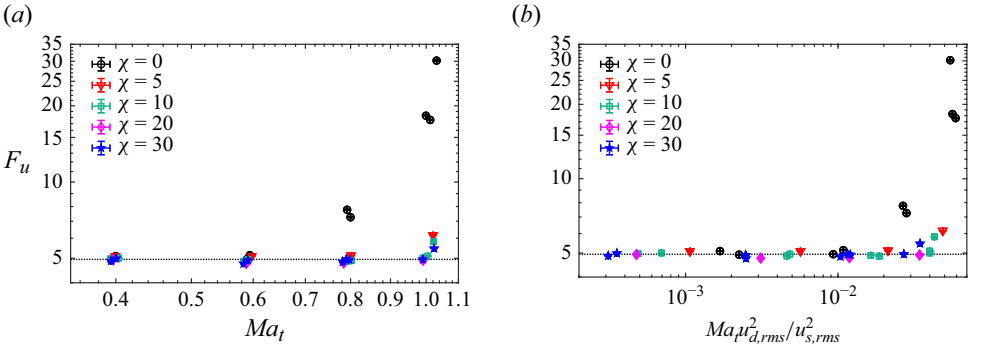

Figure 6. Flatness of the velocity gradient F_u with (*a*) Ma_t and (*b*) $Ma_t u^2_{d,rms}/u^2_{s,rms}$. The dotted line is the average value 4.95 for the cases before S_u-divergence.

the condition $Ma_t u^2_{d,rms}/u^2_{s,rms} > 3 \times 10^{-2}$ is satisfied, shocklets induce extreme values of skewness and flatness (Wang *et al.* 2011), signalling their growing influence on turbulence statistics.

Figure 5 shows the plot of S_u. For most cases without 'S_u-divergence', the mean skewness is approximately -0.460, consistent with incompressible scaling at the present Re_λ. For the different χ cases simulated here, the comparison suggests that the critical threshold for 'S_u-divergence' may increase as χ rises, and for $\chi = 30$, no divergence is observed despite the phase diagram in figure 1(*b*). Flatness, F_u (figure 6), shows a similar trend, with the mean value 4.95 for non-divergent cases. Increasing bulk viscosity suppresses shocklet-induced intermittency, indicating that sufficiently large χ restores near-incompressible statistics even at relatively high Mach numbers.

4. Discussion and conclusions

We conduct numerical simulations of forced homogeneous isotropic turbulence over varying bulk viscosities, Reynolds numbers and Mach numbers, and examine the scaling of Favre-averaged TKE (via Helmholtz decomposition), r.m.s. pressure, pressure dilatation, dilatational dissipation and higher-order velocity-gradient moments. New models are developed for pressure dilatation and for the bulk-viscosity dependence of dilatational dissipation.

Although the solenoidal and dilatational components of the Favre-averaged TKE are not strictly orthogonal, their ratio is well approximated by the squared ratio of the respective r.m.s. velocities, as confirmed numerically. The r.m.s. pressure departs from classical pseudo-sound predictions (Ristorcelli 1997) but tends towards that limit as bulk viscosity increases. It remains close to the Donzis r.m.s. pressure model (Donzis & John 2020), with the solenoidal contribution increasingly dominant at larger bulk viscosity.

For compressible dissipation, we analyse pressure dilatation and dilatational dissipation. Pseudo-sound theory is found to be inaccurate across Mach numbers. Without bulk viscosity, pressure dilatation transfers energy mainly from TKE to mean internal energy; finite bulk viscosity can reverse this transfer at high Mach numbers. Extending Zeman's (1991) approach and the Donzis pressure model (Donzis & John 2020), we propose a new pressure-dilatation model based on the velocity ratio, with improved accuracy at large bulk viscosity. For dilatational dissipation, we show that the scaling exponent in the Donzis velocity-ratio model is not universal but varies systematically with bulk viscosity, involving an amended exponent and prefactor.

We further evaluate the velocity-gradient skewness and flatness. Donzis & John (2020) identified the shocklet-induced 'S_u-divergence' as governed by the parameter $Ma_t u_{d,rms}^2/u_{s,rms}^2$. The divergence emerges once this parameter exceeds a critical threshold, but this threshold may increase with bulk viscosity; at sufficiently large bulk viscosity 'S_u-divergence' may be fully suppressed even when the empirical value is exceeded.

Overall, the velocity-ratio scaling framework offers a promising route toward universal laws for compressible turbulence. By incorporating bulk-viscosity effects, the present study refines this framework and delivers new modelling for TKE decomposition, pressure dilatation and dilatational dissipation. A natural extension is the development of separate transport equations for the solenoidal and dilatational components of TKE.

Supplementary material. Supplementary material is available at https:/doi.org/10.1017/jfm.2026.11466.

Funding. This work has been supported by the Chinese Academy of Sciences Project for Young Scientists in Basic Research (YSBR-107), the National Natural Science Foundation of China (NSFC award numbers 91852205, 42075071), NSFC Basic Science Center Program (Award number 11988102), Department of Science and Technology of Guangdong Province (2023B1212060001) and Guangdong-Hong Kong-Macao Joint Laboratory for Data-Driven Fluid Mechanics and Engineering Applications (2020B1212030001).

Declaration of interests. The authors report no conflicts of interest.

Data availability statement. The data that support the findings of this study are available from the corresponding author upon reasonable request.

References

Champagne, F.H. 1978 The fine-scale structure of the turbulent velocity field. *J. Fluid Mech.* **86** (1), 67–108.

Chen, S., Wang, X., Wang, J., Wan, M., Li, H. & Chen, S. 2019 Effects of bulk viscosity on compressible homogeneous turbulence. *Phys. Fluids* **31** (8), 085115.

Chu, B.-T. & Kovásznay, L.S.G. 1958 Non-linear interactions in a viscous heat-conducting compressible gas. *J. Fluid Mech.* **3** (5), 494–514.

Cramer, M.S. 2012 Numerical estimates for the bulk viscosity of ideal gases. *Phys. Fluids* **24** (6), 066102.

Donzis, D.A. & Jagannathan, S. 2013 Fluctuations of thermodynamic variables in stationary compressible turbulence. *J. Fluid Mech.* **733**, 221–244.

Donzis, D.A. & John, J.P. 2020 Universality and scaling in homogeneous compressible turbulence. *Phys. Rev. Fluids* **5** (8), 084609.

Helmholtz, H. 1867 LXIII. On integrals of the hydrodynamical equations, which express vortex-motion. *Lond. Edin. Dublin Phil. Mag. J. Sci.* **33** (226), 485–512.

Ishihara, T., Kaneda, Y., Yokokawa, M., Itakura, K. & Uno, A. 2007 Small-scale statistics in high-resolution direct numerical simulation of turbulence: Reynolds number dependence of one-point velocity gradient statistics. *J. Fluid Mech.* **592**, 335–366.

JOHN, J.P. & DONZIS, D.A. 2024 Strong evidence for universality in homogeneous compressible turbulence. *Phys. Fluids* **36** (10), 106121.
KOLMOGOROV, A.N. 1941*a* Dissipation of energy in the locally isotropic turbulence. *Dokl. Akad. Nauk SSSR* **32**, 16–18.
KOLMOGOROV, A.N. 1941*b* The local structure of turbulence in an incompressible viscous fluid for very high Reynolds numbers. *Dokl. Akad. Nauk SSSR* **30**, 301–305.
KOVÁSZNAY, L.S.G. 1953 Turbulence in supersonic flow. *J. Aeronaut. Sci.* **20** (10), 657–674.
LI, C., YANG, Y., MATTHAEUS, W.H., JIANG, B., WAN, M. & CHEN, S. 2024 Non-universality and dissipative anomaly in compressible magnetohydrodynamic turbulence. *J. Fluid Mech.* **992**, A9.
PAN, S. & JOHNSEN, E. 2017 The role of bulk viscosity on the decay of compressible, homogeneous, isotropic turbulence. *J. Fluid Mech.* **833**, 717–744.
PETERSEN, M.R. & LIVESCU, D. 2010 Forcing for statistically stationary compressible isotropic turbulence. *Phys. Fluids* **22** (11), 116101.
POPE, S.B. 2000 *Turbulent Flows*. Cambridge University Press.
QI, Y., WANG, L.-P., GUO, Z. & CHEN, S. 2023 Consistent lifting relations for the initialization of total-energy double-distribution-function kinetic models. *Phys. Rev. E* **108** (6), 065301.
RISTORCELLI, J.R. 1995 A pseudo-sound constitutive relationship for the dilatational covariances in compressible turbulence: an analytical theory. *ICASE Rep.* 95-22. NASA Langley Research Center.
RISTORCELLI, J.R. 1997 A pseudo-sound constitutive relationship for the dilatational covariances in compressible turbulence. *J. Fluid Mech.* **347**, 37–70.
RISTORCELLI, J.R. & BLAISDELL, G.A. 1997 Validation of a pseudo-sound theory for the pressure-dilatation in DNS of compressible turbulence. Report NASA/CR-201748. Institute for Computer Applications in Science and Engineering.
RUBINSTEIN, R. & CLARK, T.T. 2017 'Equilibrium, and 'non-equilibrium, turbulence. *Theor. Appl. Mech. Lett.* **7** (5), 301–305.
SAKURAI, Y. & ISHIHARA, T. 2023 Direct numerical simulations of compressible isothermal turbulence in a periodic box: Reynolds number and resolution-level dependence. *Phys. Rev. Fluids* **8** (8), 084606.
SAKURAI, Y. & ISHIHARA, T. 2024 Direct numerical simulations of compressible turbulence in a periodic box: effect of isothermal assumptions on turbulence statistics. *Phys. Fluids* **36** (8), 085152.
SAMTANEY, R., PULLIN, D.I. & KOSOVIĆ, B. 2001 Direct numerical simulation of decaying compressible turbulence and shocklet statistics. *Phys. Fluids* **13** (5), 1415–1430.
SARKAR, S. 1992 The pressure-dilatation correlation in compressible flows. *Phys. Fluids A: Fluid Dyn.* **4** (12), 2674–2682.
SARKAR, S., ERLEBACHER, G., HUSSAINI, M.Y. & KREISS, H.O. 1991 The analysis and modelling of dilatational terms in compressible turbulence. *J. Fluid Mech.* **227**, 473–493.
SUTHERLAND, W. 1893 LII. The viscosity of gases and molecular force. *Lond. Edinb. Dublin Phil. Mag. J. Sci.* **36** (223), 507–531.
WANG, J., GOTOH, T. & WATANABE, T. 2017 Spectra and statistics in compressible isotropic turbulence. *Phys. Rev. Fluids* **2** (1), 013403.
WANG, J., SHI, Y., WANG, L.-P., XIAO, Z., HE, X. & CHEN, S. 2011 Effect of shocklets on the velocity gradients in highly compressible isotropic turbulence. *Phys. Fluids* **23** (12), 125103.
WANG, J., WANG, L.P., XIAO, Z., SHI, Y. & CHEN, S. 2010 A hybrid numerical simulation of isotropic compressible turbulence. *J. Comput. Phys.* **229** (13), 5257–5279.
ZEMAN, O. 1991 On the decay of compressible isotropic turbulence. *Phys. Fluids A: Fluid Dyn.* **3** (5), 951–955.